The 10th International Symposium on Virtual Reality, Archaeology and Cultural Heritage VAST (2009)
K. Debattista, C. Perlingieri, D. Pitzalis, and S. Spina (Editors)

Optimized Image Sampling for View and Light Interpolation

Prabath Gunawardane[1] , Oliver Wang[1] , Steven Scher[1] , Ian Rickards[1] , James Davis[1] and Tom Malzbender[2]

[1]University of California Santa Cruz
[2]Hewlett-Packard Laboratories

Abstract

Accurate virtual reconstruction of real world objects has long been a desired goal of image-based computer graphics. Usually this involves a lengthy capture process where an object is photographed from different viewpoints and illumination conditions. Using this collection of input images, we can now re-render the object from any viewing angle or lighting condition. However, acquiring a dense sampling of both the lighting and view space is time consuming. We carry out an analysis on this combined lighting and view space to find the optimal sampling given a restricted image budget. We also analyze the order of interpolation and find that improved results are obtained by interpolating first in viewpoint and second in lighting, the reverse of the usual order.

Categories and Subject Descriptors (according to ACM CCS): I.4.1 [Image Processing and Computer Vision]: Digitization and Image Capture—

1 Introduction

Acquisition time is one of the key limiting factors preventing digital scanning of many real world objects for use in computer graphics. This is particularly relevant to cultural heritage preservation, since many museums have millions of artifacts they would like to document and later visualize.

Image based rendering and 3D scanning are both widely used for displaying real world objects in virtual settings. This work considers image based rendering methods because they currently offer greater photographic realism across a broader range of objects. The most common approaches either capture a large set of images under many lighting angles and then interpolate to recreate any lighting condition, or capture a large set of images from many viewing angles and then interpolate to recreate any view. Quality is typically improved by increasing the number of samples available for interpolation. Relatively few practical systems have attempted to interpolate both lighting and viewpoints because the total number of images required to exhaustively sample this joint space is very large [ECJ*06].

The key challenge is to reduce the number of photographic image samples that need to be acquired while preserving the power of our digital model to aesthetically represent the object and allow reliable analysis. But which image samples should we take to optimally represent both views and lighting? And can our methods for interpolation be improved if both view and lighting information is available?

The primary contributions of this paper are analysis and experiments that answer the following important interpolation decisions:

- What order of lighting model should be used to achieve the most accurate reconstruction when a limited number of lighting conditions are captured?
- When interpolating both view and lighting, what is the optimal tradeoff between view and lighting sampling for a limited total number of images?
- When interpolating both view and lighting, should interpolation be performed in lighting first, and then in viewpoint, or vice-versa?

2 Related Work

View Interpolation View interpolation relies on knowing pixelwise correspondences between images, stored as the depth at each pixel, or as flow vectors between images [CW93] [SD95] [AS97]. A good survey is available [SK00]. Flow estimation can be improved by grouping pixels [ZKU*04], introducing proxy geometry [DBY98], or even building a 3D model [SD99].

Capturing a 4D Lightfield allows view synthesis without determining correspondences, but acquisition time is prohibitively long [LH96] [CCST00] [GZC*06]. Estimat-

© The Eurographics Association 2009.

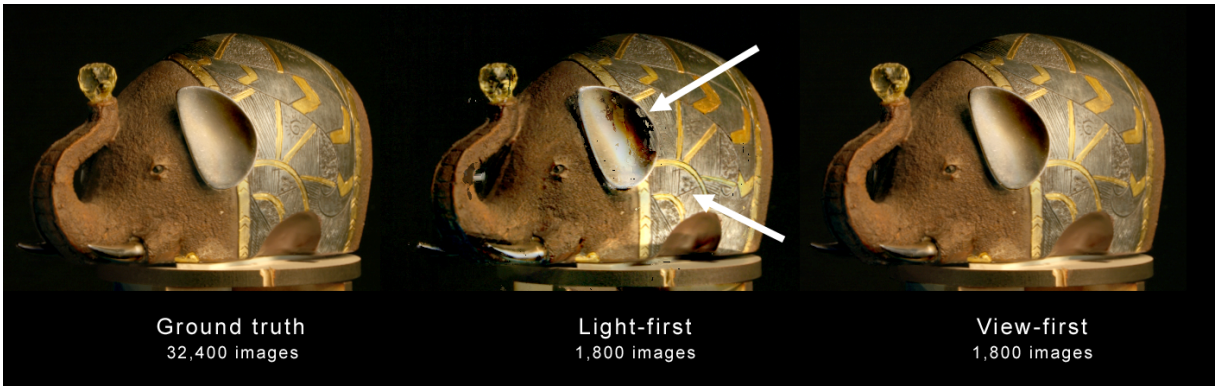

Figure 1: *Joint lighting and view interpolation may suffer from noticeable artifacts. Notice the blotches inside the elephant's ear and the incorrect position of the specular highlight on the side of the body. View-first interpolation, the reverse of the traditional light-first order, produces substantially better renderings with the same number of images.*

ing proxy geometry gives better estimates of scene flow [GGSC96]. Buehler et al. proposed an approach which ties together these techniques to create a generalized image-based rendering framework [BBM*01].

Lighting interpolation Most practical relighting techniques capture samples of a 2D slice of the complete BRDF, with the viewpoint fixed. Interpolation may assume a linear [DHT*00], polynomial [MGW01], spherical harmonic [SKS02], or wavelet [NRH04] [WTL05] model. Maselus et al. [MPDW04] compare several interpolation functions. Fuchs et al. [FLBS07] use image-based priors to generate super-resolution reflectance fields, simulating a dense lighting sampling with a sparser set. To overcome the interpolation issues posed by self-shadowing, Matsushita et al. propose using shadow masks generated via surface geometry and lighting information [MKL*02] .

Relighting can also be achieved by measuring the surface normals and the full BRDF for each surface point. This could be represented as a 2D surface lightfield [WAA*00], or as a 4D BRDF; a good survey of BRDF capture techniques is available [MMS*05]. The number of lighting samples required can be reduced by theoretical analysis of the sampling density [LWS02], assuming smooth BRDF variation [REB06], or clustering material types [LKG*03].

Joint View *and* Lighting Interpolation An extremely dense sampling will capture the entire 8D light field with no assumptions of 3D geometry, but is prohibitively time consuming [GTLL06]. At the other extreme, an object's 3D shape and BRDF can be captured [MWL*99] and rendered to its surface [YXA07]. Even without measuring the full BRDF, many joint interpolation techniques use an explicit 3D model, taken from the visual hull [VHC06] [MPN*02], a range scanner [LKG*03], or photometric stereo [HS05].

The USC LightStage project captured multiview relighting data [ECJ*06] and applied "light-first" interpolation as described in the next section. View interpolation preprocessing prior to lighting interpolation has been used to account for undesired motion artifacts [WGT*05] [ECJ*06], but has not been analyzed or applied to increase robustness in joint view and lighting interpolation. This paper presents the first such analysis of the effects of interpolation ordering in this joint space.

3 Experimental Setup

We photograph objects in a hemispherical dome with 64 lights (figure 2). At the center of the dome, the target object sits on a turntable accurate to more than .01 degrees. The camera is geometrically and radiometrically calibrated [Zha99]. An array of cameras could have allowed 2D image interpolation, but 1D view interpolation and 2D view interpolation present the same research challenges.

Our lights are halogen bulbs which we have measured to reach full intensity approximately 1 second after power is applied. We have verified that light output is consistent even after many on/off cycles. To ensure completely repeatable light intensity and color temperature we take one image every 2 seconds. The current camera, an 8Mpix Canon Rebel XT DSLR, downloads a photograph to the host computer in approximately 1 second. A "complete" capture session consists of cycling through all 64 lights at 1 degree increments, for a total of 23,040 images, or 13 hours and 185 GB of data.

4 Background

4.1 Lighting Interpolation

The images of a scene at a stationary viewpoint will obviously change if the lighting is moved. Figure 3 shows an example of a single pixel's color changing as the light is moved. Both the surface BRDF and cast shadows can cause sudden changes to the observed color from a small change in illumination direction. Nevertheless, it is common and desirable to treat the BRDF as a continuous model, in order to smoothly render views of the scene with lighting from a novel direction. Two such common interpolation functions used for representing BRDFs are spherical harmonics (SH) and polynomial texture maps (PTM) [MGW01] [SKS02]

The choice of lighting model leads to a visually noticeable change in an image rendered from the same input im-

© The Eurographics Association 2009.

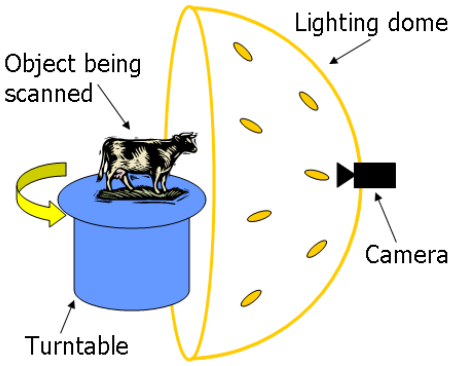

Figure 2: *The capture device used in this work consists of an DSLR camera, a rotational platform, and 64 controllable lights.*

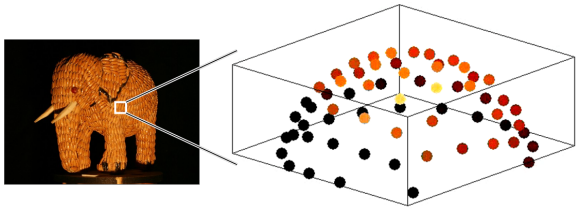

Figure 3: *The reflectance data for a single pixel is captured from a hemisphere of different lighting directions. This sparse data must be fit to an interpolation function to render smooth relighting.*

ages, as Figure 4 illustrates. Notice that for this object, using the 9-coefficients SH model gives a substantially improved perception of "shininess" and lower error residual than the 6-parameter PTM. A higher-order model might increase quality further, but might also cause artifacts due to over fitting if the number of captured images is too low. In the cultural heritage community, use of low order PTMs dominates. In the computer vision academic community, use of SH dominates. For the remainder of this paper, we choose to analyze SH.

Consider several images taken from the same viewpoint, with different lighting conditions. Two angles, θ and ϕ, describe the incoming light direction and define the vector $\vec{\mathbf{a}}$ by Equation (1). All such vectors, representing images with different light directions, may be stacked into a matrix $\mathbf{A} = [\vec{\mathbf{a}}_1, \vec{\mathbf{a}}_2, ...]^T$. Similarly, the brightnesses c_i from each image i at pixel p may be stacked into a vector $\vec{\mathbf{b}}(p) = [c_1(p), c_2(p), ...]^T$. The SH coefficients $\vec{\mathbf{x}}(p)$ may be found with Equation (2), and the interpolated brightness $y(p)$ under a new lighting direction $\vec{\mathbf{a}}_{new}$ with Equation (3).

$$\vec{\mathbf{a}} = [1, sin(\theta)sin(\phi), cos(\theta), cos(\phi)sin(\theta), ...]^T \quad (1)$$

$$\mathbf{A} * \vec{\mathbf{x}}(p) = \vec{\mathbf{b}}(p) \quad (2)$$

$$y(p) = \vec{\mathbf{a}}_{new}^T * \vec{\mathbf{x}}(p) = \vec{\mathbf{a}}_{new}^T * \mathbf{A}^{-1} * \vec{\mathbf{b}}(p) \quad (3)$$

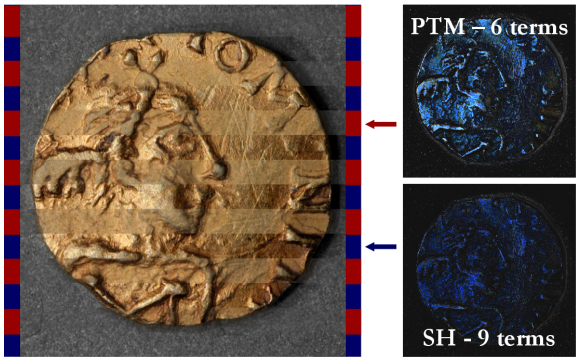

Figure 4: *The number of coefficients in the lighting interpolation function matters. Polynomial Texture Maps with 6 coefficients are compared against Spherical Harmonics with 9 coefficients in alternating stripes. Using more terms clearly increases the perception of shininess. The contrast enhanced error residuals on the right confirm that additional terms reduce error.*

4.2 View Interpolation

If several images are captured at distinct viewpoints and registered to one another via optical flow (or stereo matching), image-based rendering may be used to synthesize a new image of the scene from a novel viewpoint. This may be done by simply warping each image to the new viewpoint and averaging, as in Equation (4). Here, $c_i(p)$ is the brightness of the image at the i^{th} viewpoint at pixel p, and F_i is the correspondence function for viewpoint i that maps pixel p in the novel view to pixel $F_i(p)$ in image i. A gaussian weighting w_i is centered at the new view.

$$y(p) = \sum_i (w_i * c_i(F_i(p))) \quad (4)$$

Optical flow robustness has been previously reported as a challenge in this domain [ECJ*06]. In addition to images with a single light source active, we capture frames at each view with all lights active, providing better optical flow estimation [OA05]. Nevertheless, as viewpoint spacing gets too wide, the displacement vectors lose robustness and view interpolation artifacts result.

4.3 Joint Lighting and View Interpolation

Joint view and lighting interpolation has traditionally been achieved by "light-first" interpolation, as shown in figure 5(a). This consists of fitting the lighting model separately to each viewpoint, calculating a relit image at each viewpoint, and then applying view interpolation to the relit images. This equates to solving several small sets of linear equations separately, and averaging the results, as in Equation (5). As before, the vector $\vec{\mathbf{b}}_i$ stacks brightnesses from all lighting conditions at the i^{th} viewpoint, and the matrix $\mathbf{A_i}$ stacks the lighting direction vectors $\vec{\mathbf{a}}^T$ from each lighting condition at the i^{th} viewpoint.

$$y(p) = \sum_i (\vec{\mathbf{a}}_{new}^T * \mathbf{A_i}^{-1} * w_i * \vec{\mathbf{b}}_i(F_i(p))) \quad (5)$$

© The Eurographics Association 2009.

The alternative "view-first" interpolation reverses the order of interpolation, as in Equation (6). All images are warped to the new viewpoint, a single lighting model is fit to the entire collection of warped images, and a new image is rendered under novel lighting. To do this, the brightness vectors $\vec{\mathbf{b}}_i$ and matrices from every viewpoint – each containing brightnesses under all lighting conditions – are stacked together, yielding a single, large set of equations to solve.

$$y(p) = \vec{\mathbf{a}}_{new}^{T} * \begin{pmatrix} \mathbf{A_1} \\ \mathbf{A_2} \\ \dots \\ \mathbf{A_n} \end{pmatrix}^{-1} * \begin{pmatrix} w_1 * \vec{\mathbf{b}}_1(F_1(p)) \\ w_2 * \vec{\mathbf{b}}_2(F_2(p)) \\ \dots \\ w_n * \vec{\mathbf{b}}_n(F_n(p)) \end{pmatrix} \quad (6)$$

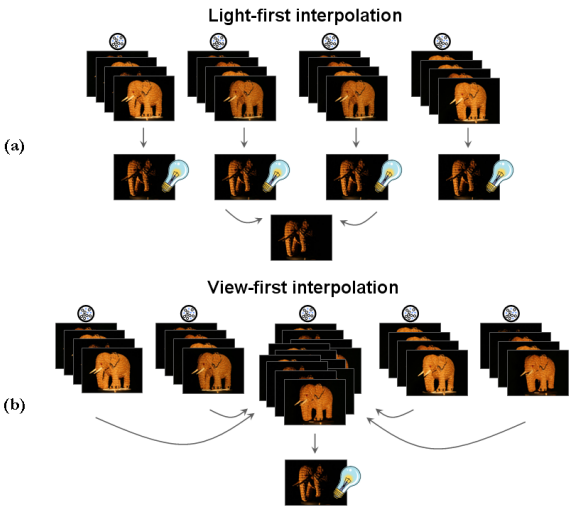

Figure 5: *Joint view and light interpolation has traditionally been accomplished using Light-first interpolation.* First, *the lighting conditions at each view are interpolated to compute a relit image, and* then *a flow field is used to warp the relit images to the final viewing position. This paper proposes View-first interpolation.* First, *a flow field warps the raw images to the final viewing position,* then *the entire resulting stack of images is light interpolated to create the final relit image.*

5 Optimal Image Budget Allocation Analysis

A more complex lighting model provides greater fidelity as long as enough images are available to avoid noise from under-fitting. We determine the optimal model complexity for a given number of input lighting conditions.

Both lighting and view interpolation are subject to errors often ameliorated by capturing more images. Given a limited number of total images to capture, we determine the optimal balance of viewpoints and lighting conditions that maximizes image quality.

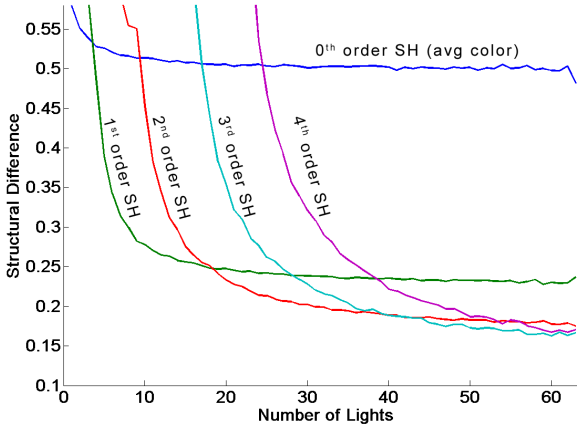

Figure 6: *When more lighting conditions are available, the structural difference error decreases. Spherical harmonic light interpolation functions of several orders are shown; for a given budget of lighting images, the order with the lowest error should be chosen.*

5.1 Optimal Lighting Model

The choice of lighting models can greatly affect image quality, as demonstrated earlier in Figure 4. The optimal choice would try to use a complex model to capture maximum detail while avoiding underfitting. Since a spherical harmonic model of order N has $(N+1)^2$ coefficients, at least this many images are required for a reasonable fit. How many more? We now investigate the best model for a given number of input images.

We captured 64 images of a wooden elephant from a single viewpoint using the 64 lighting directions. These images were repeatedly divided into disjoint training and test sets of varying sizes. Several spherical harmonic models of different complexities were fit to the training set and used to predict the observed brightness in the test set. The results of this experiment are given in Figure 6. Errors are reported as Structural Difference, defined as the complement to the Structural Similarity perceptual error metric [WBSS04]. The mean square error behaves similarly. Each line corresponds to a spherical harmonic model of a different order.

The major trends are as expected: capturing more lighting conditions allows a better fit that reduces error, a higher-order model allows a lower error if enough lighting samples are available, and the best results are obtained using all the lights and a high order model.

The lighting model can now be tailored to the image budget. For example, if an image budget of only 25 images is available, we can see that a 2nd order harmonic with 9 terms provides the lowest error. Importantly, increasing the model complexity provides diminishing returns.

The visual manifestation of "error" in figure 6 is made clear in figure 7, which compares images rendered using a 2nd order spherical harmonic fit to different numbers of lights. When using only 12 lights, the fit is not robust and the

© The Eurographics Association 2009.

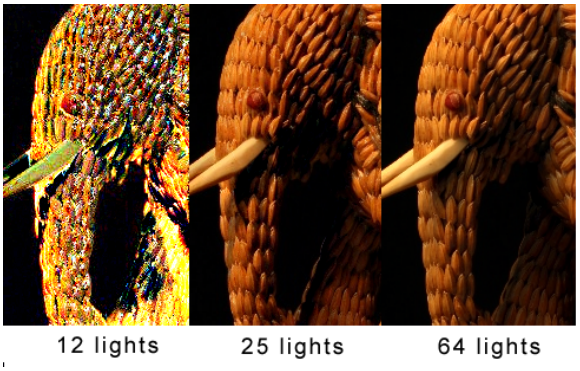

Figure 7: *For the same lighting model, too few lights cause underfitting, with very large errors that appear as objectionable high frequency pixel noise. Using a sufficient number of lights removes such errors, and even more lights give a smaller increase in detail.*

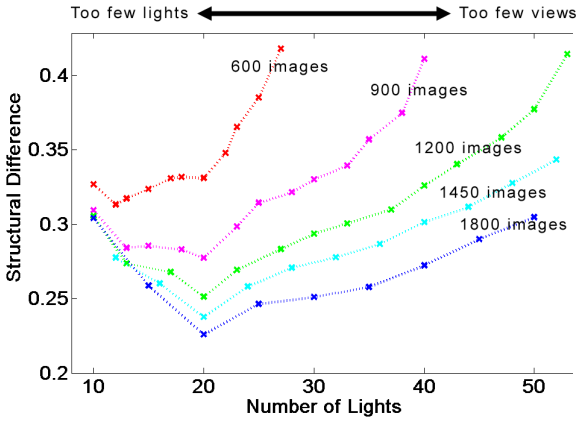

Figure 8: *There is a tradeoff between sampling lighting conditions and sampling viewpoints. Using too few lights at each viewpoint increases error, as does using too few viewpoints.*

relatively high error manifests itself as objectionable high frequency pixel noise. Using 64 lights provides the highest quality fit possible using our device. Using 25 lights has higher error than 64 lights, but the fitting process is robust and the error manifests itself primarily as change of sharpness in highlight and shadow regions. This is perceptually acceptable to our visual system since it can be understood as a change in illumination, and most viewers will not object.

5.2 Balancing Light and View Sampling

Reducing the number of sampled images forces a tradeoff between capturing additional viewpoints, or capturing more lighting conditions at each viewpoint. Wide separations between adjacent viewpoints lead to view interpolation error, while too few lighting conditions cause lighting interpolation errors. This leads to a dilemma: for reasonable image budgets, it is impossible to obtain a large number of samples for both views and lights.

We experimentally determine the optimal balance by measuring the total error of joint interpolation for a range of viewpoints and lighting conditions. Images of a vase were captured at all 64 lighting conditions, at every viewpoint over 360 degrees in 1-degree increments. In our experiment, we take a subset of these images with the indicated number of lighting conditions used at each viewpoint, and with viewpoints evenly distributed over 360 degrees. For a given number of lighting conditions, the spherical harmonic model order is chosen according to figure 6.

This experiment applies the “light-first" approach common in the literature, as described in the previous section. Images from a pair of adjacent viewpoints in the subset are used to generate novel images at a new lighting direction, and view interpolation is performed between these two images to render a novel view at a viewpoint midway between them. This is repeated for all adjacent image pairs, for all lighting conditions not in the subset. The plot shown here uses structural difference as an error metric; mean squared error gives qualitatively similar results.

As expected, that the lowest error occurs when the needs of view and lighting interpolation are balanced, as Figure 8 shows. The minimum point of the curve is object dependant; this plot was made with the vase dataset shown in figure 9. We have found the curves to have a similar “U" shape across all of our experimental objects, but to favor more lighting conditions for very shiny objects.

Several points in the design space may be compared visually in Figure 9. A sparse set of 36 views, each with a large set of 50 lighting conditions, results in artifacts during view interpolation, since there are too few views. Notice in particular the tearing on the lion’s body.

Using 180 densely-spaced viewing conditions results in smooth view interpolation, however the resulting 10 lights per view are too few samples, leading to artifacts while relighting. In this case the shadowing is noticeably too dark near the top of the lion, and the specular highlight near the diamond is incorrect. When enough samples are available, choosing a balance between view and light sampling provides acceptable image quality. In this case using 90 views and 20 lights is the minimum error tradeoff, and the image has no apparent artifacts. However when a budget of only 900 images is available, even the tradeoff with lowest possible error (at 45 views and 20 lights) is noticeably flawed. Notice the tearing near the back leg of the lion.

We find that 20 lights are typically optimal when using light-first interpolation for the objects we capture. Previous work with different subjects (e.g. people) have used 30 lighting conditions at 10 degree viewpoint separation [ECJ*06] and 60 lighting conditions and 10-degree viewpoint separation [MPN*02].

© The Eurographics Association 2009.

Figure 9: *Interpolating between too few views results in artifacts, as does interpolating between too few lights. Choosing the optimal tradeoff between lights and views results in interpolation with no visible errors. If the image budget is too small, even the optimal tradeoff will contain noticeable artifacts.*

6 Light and View Interpolation Analysis

As discussed in the Background section, joint lighting and view interpolation is typically achieved in a "light first" order. In this section, we experimentally compare this approach to the alternative "view first" interpolation order, and investigate implications for the optimal image budget balance discussed in the previous section.

For each method, we use the same total number of images, but in a different configuration tailored to each option. For the light-first case, we use the optimal balance as determined by Figure 8. Note that using light-first interpolation with any other balance would give worse results. View-first interpolation has a different optimal balance, with view separations four times as close.

For view-first interpolation, a different set of lights are used at neighboring viewpoints, which allows a higher-order model to be fit since lights are shared between several viewpoints. This is not possible for light-first interpolation because ghosting appears in shadowed and specular regions.

Many graphics applications require completely arbitrary view locations. Though view-first interpolation samples from many (e.g. eight) viewpoints to render a result, its best results are obtained when the target viewpoint is included as one of the sampled viewpoints. Since the optimal view/light tradeoff for view-first interpolation prefers dense viewpoint sampling (e.g. one degree), in practice we only render at sampled viewpoints. Note that images from all viewpoints but one must still be warped to the target view.

6.1 Quantitative Comparison

Dataset	Struc. Diff.		RMSE	
	View 1st	Light 1st	View 1st	Light 1st
Elephant 1	0.04	0.15	3.62	13.00
Vase	0.03	0.18	4.93	15.30
Silver Box	0.08	0.18	5.61	10.82
Elephant 2	0.02	0.05	2.23	2.53
Lion	0.04	0.16	4.12	13.00

Figure 10: *Light-first interpolation was compared to view-first interpolation using both structural difference and root mean square error. In all cases view-first interpolation produced lower error. The same total number of images was used for each interpolation method.*

An object was imaged at 1-degree viewpoint increments and all 64 lighting conditions. At each viewpoint, all 64 lights were used to fit a spherical harmonic lighting model. This model was used to render a relit image at this view under a novel lighting direction; this image is considered the "ground truth". This process is repeated for several objects.

A subset of images was used to evaluate each interpolation method: 20 lights at large view increments for light-first interpolation, and 5 lights at small view increments for view-first; for the view-first case, different lights were used at each view, repeating after 8 views, for 40 lighting conditions. The light-first method used 20 images at each of 2 viewpoints adjacent to the target view, warping all images to the target view. The view-first method used 5 images at each of 8 viewpoints. One viewpoint already was the target view, and the seven closest viewpoints are warped to the target view. In both cases, the rendered image was compared to the "ground truth" obtained using all 64 lights at the target view.

The error was evaluated for all 360 viewpoints, with a different novel lighting direction at each view. The Structural Difference is averaged over these 360 cases, and reported for several objects in figure 10.

6.2 Visual Comparison

Figure 1 shows an example of joint view and light interpolation. Note that view-first interpolation produces fewer artifacts than light-first interpolation. In particular light-first

© The Eurographics Association 2009.

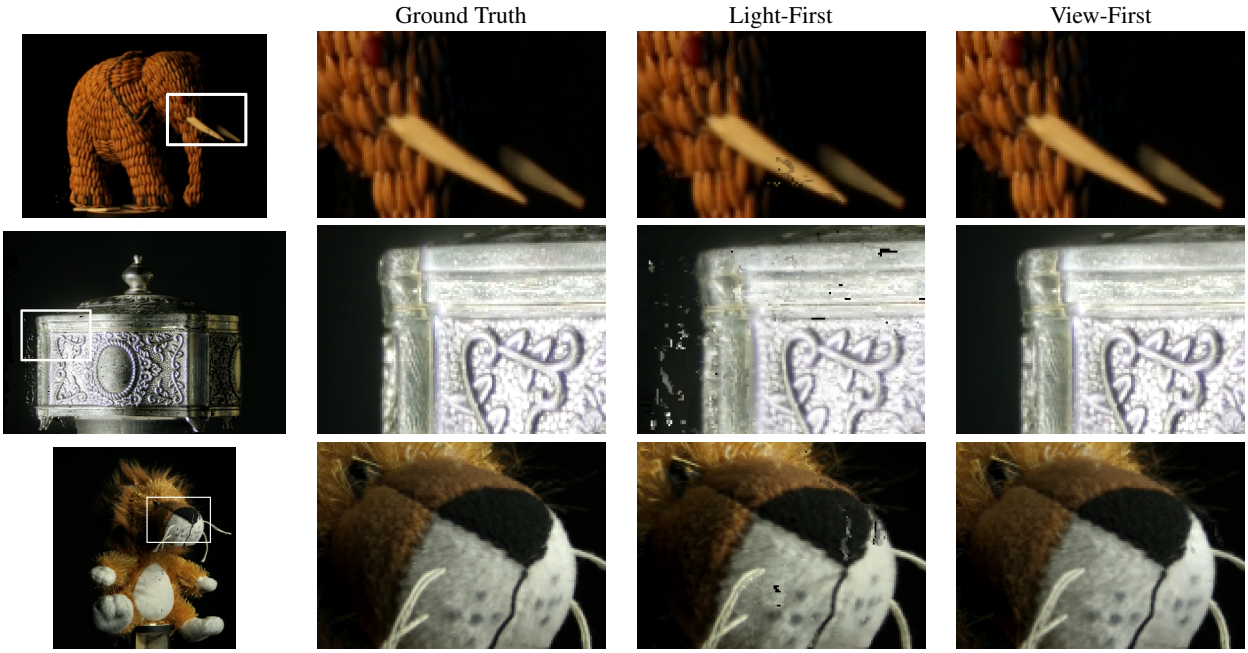

Figure 11: *Comparisons of ground truth, light-first, and view-first interpolation, as described in Section 6.1. In all cases light-first interpolation suffers small artifacts due to erroneous flow vector estimates. View-first interpolation is very close to ground truth.*

interpolation produces blotches inside the elephant's ear due to wrong flow vectors, as well as incorrect positioning of the specular highlight on the side of the body. We hypothesize that the highlight position error is caused by the fact that light-first interpolation has access to only 20 lighting conditions, while view-first interpolation uses light sharing to gain access to 40 light conditions.

Several more comparison examples are presented in Figure 11. The zoomed out regions show the artifacts due to light-first view interpolation. This shows that view-first interpolation improves the reconstruction results perceptually as well as numerically.

7 Discussion

Our analysis provides two benefits. Firstly, maximal image quality can be obtained by choosing the optimal lighting model order, and the optimal view/lighting sampling tradeoff. In practice, capturing a full set of lighting conditions at a few adjacent viewpoints will suffice to generate object-specific copies of figures 6 and 8, from which optimal parameters may be found for use in the whole 360-degree capture. This process is fully automatic, but may often be unnecessary since many similar objects are typically captured, so the optimum will be the same for all of them.

Secondly, we observe that view-first interpolation produces fewer artifacts than light-first interpolation with the same image budget. This is due to how errors in the flow vectors propagate in the two different methods.

With light-first interpolation, errors in flow vectors cause pixels to move to incorrect positions in the resulting image. This causes tearing artifacts and structural discontinuities which are immediately obvious to our perception.

With view-first interpolation, errors in flow vectors simply cause the BRDF to be sampled from a different point on the surface of the object. Most material reflectance acts as a low-pass filter in lighting space (meaning that a large component of reflection is often diffuse) and therefore, incorrect samples do not have a large effect on the final reconstructed BRDF. Furthermore, because of the way that flow vectors are often computed, erroneous points that get sampled will likely even correspond to the same material as the correct point, and therefore have very similar reflectance parameters, causing the resulting BRDF to often be very close to the correct BRDF.

8 Conclusion

Image based rendering allows photo-realistic synthesis of objects at new viewpoints and lighting conditions. Due to the simplicity of capture, it is poised to replace simple photographic archival records of many cultural heritage artifacts. Acquisition time is the primary hurdle preventing wider adoption, and the subsequent digitization of millions of artifacts.

This work presents an analysis of the tradeoff between viewpoint and light sampling that leads to a lower image sampling budget given the same quality requirements. In addition, the observation that order of interpolation is important leads to the presentation of view-first interpolation as an alternative to light-first interpolation.

© The Eurographics Association 2009.

Acknowledgments

Support for this work was provided by Cultural Heritage Imaging, UC CITRIS, LANL ISSDM, and NSF #CCF-0746690

References

[AS97] AVIDAN S., SHASHUA A.: Novel view synthesis in tensor space. In *CVPR* (1997). 1

[BBM*01] BUEHLER C., BOSSE M., MCMILLAN, GORTLER S., COHEN M.: Unstructured lumigraph rendering. In *Siggraph* (2001). 2

[CCST00] CHAI J.-X., CHAN S.-C., SHUM H.-Y., TONG X.: Plenoptic sampling. In *Siggraph* (2000). 1

[CW93] CHEN S. E., WILLIAMS L.: View interpolation for image synthesis. In *Siggraph* (1993). 1

[DBY98] DEBEVEC P., BOSHOKOV G., YU Y.: Efficient view-dependent image-based rendering with projective texture-mapping. In *Eurographics Rendering Workshop* (1998). 1

[DHT*00] DEBEVEC P., HAWKINS T., TCHOU C., DUIKER H.-P., SAROKIN W., SAGAR M.: Acquiring the reflectance field of a human face. In *Siggraph* (2000). 2

[ECJ*06] EINARSSON P., CHABERT C. F., JONES A., MA W. C., LAMOND B., HAWKINS T., BOLAS M., SYLWAN S., DEBEVEC P.: Relighting human locomotion with flowed reflectance fields. In *Eurographics Workshop on Rendering* (2006). 1, 2, 3, 5

[FLBS07] FUCHS M., LENSCH H. P. A., BLANZ V., SEIDEL H. P.: Superresolution reflectance fields: Synthesizing images for intermediate light directions. *Comp. Graph. Forum* (2007). 2

[GGSC96] GORTLER S. J., GRZESZCZUK R., SZELISKI R., COHEN M. F.: The lumigraph. In *Siggraph* (1996). 2

[GTLL06] GARG G., TALVALA E.-V., LEVOY M., LENSCH H.: Symmetric photography: Exploiting data-sparseness in reflectanec fields. In *Eurographics Symposium on Rendering* (2006). 2

[GZC*06] GEORGIEV T., ZHENG K. C., CURLESS B., SALESIN D., NAYAR S., INTWALA C.: Spatio-angular resolution tradeoffs in integral photography. In *Eurographics Workshop on Rendering* (2006). 1

[HS05] HERTZMANN A., SEITZ S. M.: Example-based photometric stereo: Shape reconstruction with general, varying BRDFs. *IEEE Transactions on Pattern Analysis and Machine Intelligence* (2005). 2

[LH96] LEVOY M., HANRAHAN P.: Light field rendering. In *Siggraph* (1996). 1

[LKG*03] LENSCH H. P. A., KAUTZ J., GOESELE M., HEIDRICH W., SEIDEL H.-P.: Image-based reconstruction of spatial appearance and geometric detail. *ACM Trans. Graph.* (2003). 2

[LWS02] LIN Z., WONG T.-T., SHUM H.-Y.: Relighting with the reflected irradiance field: Representation, sampling and reconstruction. *Int. J. Comput. Vision* (2002). 2

[MGW01] MALZBENDER T., GELB D., WOLTERS H.: Polynomial texture maps. In *Siggraph* (2001). 2

[MKL*02] MATSUSHITA Y., KANG S. B., LIN S., SHUM H.-Y., TONG X.: Lighting interpolation by shadow morphing using intrinsic lumigraphs. In *Pacific Conference on Computer Graphics and Applications* (2002). 2

[MMS*05] MÜLLER G., MESETH J., SATTLER M., SARLETTE R., KLEIN R.: Acquisition, synthesis and rendering of bidirectional texture functions. *Computer Graphics Forum* (2005). 2

[MPDW04] MASSELUS V., PEERS P., DUTRÉ P., WILLEMS Y. D.: Smooth reconstruction and compact representation of reflectance functions for image-based relighting. In *Eurographics Workshop on Rendering* (2004). 2

[MPN*02] MATUSIK W., PFISTER H., NGAN A., BEARDSLEY P., ZIEGLER R., MCMILLAN L.: Image-based 3D photography using opacity hulls. *ACM Trans. Graph.* (2002). 2, 5

[MWL*99] MARSCHNER S. R., WESTIN S. H., LAFORTUNE E. P., TORRANCE K. E., GREENBERG D. P.: Image-based brdf measurement including human skin. In *Eurographics Workshop on Rendering* (1999). 2

[NRH04] NG R., RAMAMOORTHI R., HANRAHAN P.: Triple product wavelet integrals for all-frequency relighting. In *Siggraph* (2004). 2

[OA05] OGALE A. S., ALOIMONOS Y.: Shape and the stereo correspondence problem. *Int. J. Comput. Vision* (2005). 3

[REB06] RAMAMOORTHI R., ENRIQUE S., BELHUMEUR P. N.: Reflectance sharing: Predicting appearance from a sparse set of images of a known shape. *IEEE Trans. Pattern Anal. Mach. Intell.* (2006). 2

[SD95] SEITZ S. M., DYER C. R.: Physically-Valid View Synthesis by Image Interpolation. In *Workshop on Representation of Visual Scenes* (1995). 1

[SD99] SEITZ S., DYER C.: Photorealistic scene reconstruction by voxel coloring. *Int. J. Comput. Vision* (1999). 1

[SK00] SHUM H., KANG S.: A review of image-based rendering techniques. In *IEEE/SPIE Visual Communications and Image Processing* (2000). 1

[SKS02] SLOAN P.-P., KAUTZ J., SNYDER J.: Precomputed radiance transfer for real-time rendering in dynamic, low-frequency lighting environments. *ACM Trans. Graph.* (2002). 2

[VHC06] VOGIATZIS G., HERNANDEZ C., CIPOLLA R.: Reconstruction in the round using photometric normals and silhouettes. In *CVPR* (2006). 2

[WAA*00] WOOD D. N., AZUMA D. I., ALDINGER K., CURLESS B., DUCHAMP T., SALESIN D. H., STUETZLE W.: Surface light fields for 3D photography. In *Siggraph* (2000). 2

[WBSS04] WANG Z., BOVIK A., SHEIKH H., SIMONCELLI E.: Image quality assessment: From error measurement to structural similarity. *IEEE Trans. Image Processing* (2004). 4

[WGT*05] WENGER A., GARDNER A., TCHOU C., UNGER J., HAWKINS T., DEBEVEC P.: Performance relighting and reflectance transformation with time-multiplexed illumination. *ACM Trans. Graph.* (2005). 2

[WTL05] WANG R., TRAN J., LUEBKE D.: All-frequency interactive relighting of translucent objects with single and multiple scattering. *ACM Trans. Graph.* (2005). 2

[YXA07] YU T., XU N., AHUJA N.: Shape and view independent reflectance map from multiple views. *Int. J. Comp. Vision* (2007). 2

[Zha99] ZHANG Z.: Flexible camera calibration by viewing a plane from unknown orientations. *ICCV* (1999). 2

[ZKU*04] ZITNICK C. L., KANG S. B., UYTTENDAELE M., WINDER S., SZELISKI R.: High-quality video view interpolation using a layered representation. *ACM Trans. Graph.* (2004). 1

© The Eurographics Association 2009.